



Article

Combined Use of TiO₂ Nanoparticles and Biochar Produced from Moss (*Leucobryum glaucum* (Hedw.) Ångstr.) Biomass for Chinese Spinach (*Amaranthus dubius* L.) Cultivation under Saline Stress

Ivan Širić ¹, Sadeq K. Alhag ², Laila A. Al-Shuraym ³, Boro Mioč ¹, Valentino Držaić ¹, Sami Abou Fayssal ^{4,5}, Vinod Kumar ⁶, Jogendra Singh ⁶, Piyush Kumar ⁷, Rattan Singh ⁸, Rakesh Kumar Bachheti ^{9,10}, Madhumita Goala ¹¹, Pankaj Kumar ^{6,12,*} and Ebrahim M. Eid ^{13,*}

- ¹ University of Zagreb, Faculty of Agriculture, Svetosimunska 25, 10000 Zagreb, Croatia
 - ² Biology Department, College of Science and Arts, King Khalid University, Muhayl Asser 61913, Saudi Arabia
 - ³ Biology Department, Faculty of Science, Princess Nourah bint Abdulrahman University, Riyadh 12834, Saudi Arabia
 - ⁴ Department of Agronomy, Faculty of Agronomy, University of Forestry, 10 Kliment Ohridski Blvd, 1797 Sofia, Bulgaria
 - ⁵ Department of Plant Production, Faculty of Agriculture, Lebanese University, Beirut 1302, Lebanon
 - ⁶ Agro-Ecology and Pollution Research Laboratory, Department of Zoology and Environmental Science, Gurukula Kangri (Deemed to Be University), Haridwar 249404, India
 - ⁷ Department of Science, Vivek College of Education, Moradabad Road, Bijnor 246701, India
 - ⁸ Department of Food Technology, Guru Jambheshwar University of Science & Technology, Hisar 125001, India
 - ⁹ Department of Industrial Chemistry, College of Applied Sciences, Addis Ababa Science and Technology University, Addis Ababa P.O. Box 16417, Ethiopia
 - ¹⁰ Department of Allied Sciences, Graphic Era Hill University, Dehradun 248002, India
 - ¹¹ Department of Environment Science, Graphic Era (Deemed to be University), Dehradun 248002, India
 - ¹² Research and Development Division, Society for AgroEnvironmental Sustainability, Dehradun 248007, India
 - ¹³ Botany Department, Faculty of Science, Kafrelsheikh University, Kafr El-Sheikh 33516, Egypt
- * Correspondence: rs.pankajkumar@gkv.ac.in (P.K.); ebrahim.eid@sci.kfs.edu.eg (E.M.E.)



Citation: Širić, I.; Alhag, S.K.; Al-Shuraym, L.A.; Mioč, B.; Držaić, V.; Abou Fayssal, S.; Kumar, V.; Singh, J.; Kumar, P.; Singh, R.; et al.

Combined Use of TiO₂ Nanoparticles and Biochar Produced from Moss (*Leucobryum glaucum* (Hedw.) Ångstr.) Biomass for Chinese Spinach (*Amaranthus dubius* L.) Cultivation under Saline Stress. *Horticulturae* **2023**, *9*, 1056. <https://doi.org/10.3390/horticulturae9091056>

Academic Editor: Alberto Pardossi

Received: 22 August 2023

Revised: 15 September 2023

Accepted: 18 September 2023

Published: 21 September 2023



Copyright: © 2023 by the authors. Licensee MDPI, Basel, Switzerland. This article is an open access article distributed under the terms and conditions of the Creative Commons Attribution (CC BY) license (<https://creativecommons.org/licenses/by/4.0/>).

Abstract: Salinity-induced soil degradation poses a significant challenge to agricultural productivity and requires innovative crop-management strategies. In this study, the synergistic effect of biochar and TiO₂ nanoparticles (NPs) obtained from moss (*Leucobryum glaucum* (Hedw.) Ångstr.) biomass on the growth, yield, biochemical, and enzymatic response of Chinese spinach (*Amaranthus dubius* L.) grown under salinity stress was investigated. Purposely, *A. dubius* was grown under different combinations of arable soil, biochar, TiO₂ NPs, and saline soils. The produced biochar and TiO₂ NPs were characterized using microscopy image analysis, X-ray diffraction patterns (XRD), energy-dispersive X-ray spectroscopy (EDX), zeta potential, particle size distribution, and Fourier-transform infrared spectroscopy (FTIR). The results showed that saline stress caused a significant ($p < 0.05$) decline in growth, yield, and biochemical constituents of *A. dubius* compared to control treatments. However, the combined application of biochar and TiO₂ NPs significantly ($p < 0.05$) alleviated the saline stress and resulted in optimum fresh weight (30.81 g/plant), dry weight (4.90 g/plant), shoot and root length (28.64 and 12.54 cm), lead number (17.50), leaf area (12.50 cm²/plant), chlorophyll (2.36 mg/g), carotenoids (2.85 mg/g), and relative water content (82.10%). Biochar and TiO₂-NP application helped to reduce the levels of stress enzymes such as catalase (2.93 μmol/min/mg P), superoxide dismutase (SOD: 2.47 EU/g P), peroxidase (POD: 40.03 EU/min/g P), and ascorbate peroxidase (3.10 mM/mg P) in saline soil. The findings of this study suggest that the combination of nanotechnology and biochar derived from unconventional biomass can be a viable option to mitigate salinity-related challenges and enhance crop yield.

Keywords: circular economy; nanotechnology; pyrolysis; sustainable agriculture; saline stress

1. Introduction

Titanium dioxide (TiO₂) is a white, opaque, and naturally occurring inorganic compound; it is composed of barium cation and sulfate anion and has low toxicity and negligible biological effects [1]. This has led to the production of TiO₂ nanoparticles (TiO₂ NPs), which consist of anatase and rutile crystal forms [2]. These NPs are biocompatible, chemically stable, inexpensive, and reusable features that make them suitable for agricultural use, especially in developing countries [3]. Out of several physical and chemical methods previously employed for TiO₂-NP synthesis, chemical synthesis methods were found to have harmful environmental impacts [4]. Thus, the green synthesis method has been adopted as the most eco-friendly, sustainable, and non-expensive way to biosynthesize NPs [5]. Generally, the average TiO₂-NP size ranges between 25 and 100 nm [6], and their structure arrangement is crystalline [7]. Many studies investigated plant extracts for potential TiO₂-NP biosynthesis. For instance, the use of Aloe vera leaf extract resulted in TiO₂ NPs with large surface area and irregular size [8]. TiO₂ NPs biosynthesized from *Anona squamosa* fruit peel extract showed a spherical nature and 21–25 nm size [9]. An irregular shape and 25–110 nm particle size were obtained from the biosynthesis of TiO₂ NPs using *Catharanthus roseus* leaf extract [10]. Vimala et al. [11] biosynthesized silver NPs (AgNPs) from *Campylopus flexuosus* (Hedw.) bird moss and revealed a 58 nm particle size and −25 mV zeta potential (good stability). Iron (FeNPs) and AgNPs biosynthesized from *S. fallax* moss were spherical with 120 and 100 nm sizes, respectively [12]. However, there is very scarce information regarding the biosynthesis of TiO₂ NPs from moss biomass.

Biochar is a carbon-rich solid product resulting from the thermal conversion of unstable carbon-enriched biomass into a stable form via pyrolysis. Biochar is generally characterized by high pH, porosity, surface area, and the availability of both micro- and macrospores [13]. Agricultural, forest, and food wastes (mainly lignocellulosic biomass sources) constitute the main substrate sources used for biochar production. The latter can be a promising strategy to mitigate the increasing environmental pollution induced by disposed wastes. For instance, a recent study found that the production of biochar from spent mushroom substrate is feasible and yields a qualitative product with very few impurities [14]. Moreover, the type of substrate used directly affects the surface area of produced biochar [15]. It is worth noting that the lower the impurities in produced biochar, the higher its quality is. Moreover, pyrolysis temperature plays a key role in determining biochar physicochemical properties. Increased pyrolysis temperature results in increased pH, carbon content, structural pores, and decreased biochar yield and volatile matter [16,17].

Chinese spinach (*Amaranthus dubius* L.; Amaranthaceae) is a 30–150 cm annual plant with a branched stem, native to Central and South American regions and imported to India from Africa for around 500 years. The global amaranth market was valued at around USD 9.1 billion in 2021 and is forecasted to reach USD 21.7 billion by 2029 with a compound annual growth rate (CAGR) of 11.51% in the 2022–2029 period [18]. In India, this plant is mainly grown in the mid and high hills of the Himalayan valley; it is estimated that around 40–50 thousand hectares of *A. dubius* are grown [19]. Although it is one of the most popularly consumed leafy vegetables in India (also known as the food of the poor), accurate information related to its production and market is still scarce [20,21]. Indian cuisine has several uses of amaranth, e.g., “Raab”, which is a broth made from amaranth flour and other basic ingredients, and curries and salads (grain and fresh forms, respectively), among others. The amaranth plant is generally considered a highly tolerant crop to saline abiotic stress [22]. This is attributed to the low number of stomata of the plant, resulting in lower basal stomatal conductance [23]. Such a hypothesis was confirmed by Bellache et al. [24], who mentioned that the growth of both *A. alba* and *A. hybridus* species was severely affected at 450 and 600 mM NaCl with unpronounced effects at lower concentrations. However, a recent study [25] mentioned that this plant can be affected by saline stress at even relatively low to moderate concentrations. For instance, NaCl concentrations higher than 25 mM (50 and 100 mM) resulted in decreased growth and yield parameters due to

saline accumulation in the shoots and roots. On the other hand, antioxidant activity, total flavonoids, and total phenolics increased at 50 mM NaCl, as mentioned by Hoang et al. [25].

In the last decade, numerous studies confirmed the role of NPs in saline stress mitigation of various leafy crops, e.g., lettuce [26], cauliflower [27], alfalfa [28], and Chinese cabbage [29]. The main observed improvements were increased plant biomass, leaf chlorophyll pigment contents, and systemic acquired resistance plant defense, along with decreased leaf malondialdehyde (MDA) content. CuO and ZnO NPs application to *A. hybridus* resulted in improved plant germination rate and growth along with increased antioxidant activity within shoots and roots, as reported by Francis et al. [30]. Furthermore, the polycyclic aromatic hydrocarbon uptake by *A. tricolor* L. was reduced by around 20–55% as a result of SiO₂ NPs and ZnO NPs amendment [31]. However, no previous studies investigated the application of TiO₂ NPs on *A. dubius*. On the other hand, only a few studies evaluated the effect of biochar on *Amaranthus* spp. For instance, the amendment of *A. tricolor* L. with bamboo biochar resulted in 34.4% higher yields; however, no significant improvements were noticed in terms of plant leaf number and height [32]. The amendment of *A. tricolor* L. with biochar produced from litchi wastes resulted in increased chlorophyll pigments (chlorophyll 'a' and chlorophyll 'b') and yield and reduced leaf MDA content as reported by Jiang et al. [33]. However, no studies evaluated the potential of biochar as an amendment for *A. dubius*. The co-application of TiO₂ NPs with biochar for plant response evaluation has been scarcely investigated. To our knowledge, the co-amendment of *Sorghum bicolor* with TiO₂ NPs and biochar was the very first experiment performed. These authors reported increased chlorophyll pigments (Chl 'a' and Chl 'b') in co-treated plants compared to TiO₂ NP treated [34]. Therefore, it was evidenced from the above studies that the physiological effects can be positive and increase crop productivity and tolerance to stressful conditions [28].

Considering the aforementioned, it was hypothesized that the growth and yield characteristics of *A. dubius* grown in saline soils would be differentially affected by applying *L. glaucum* biomass-derived biochar and TiO₂ NPs, both separately and in combination. In addition, it is hypothesized that these treatments will induce different biochemical and enzymatic responses in the plant. Therefore, the current study aimed to investigate the separate and combined effects of TiO₂ NPs and biochar produced from *L. glaucum* biomass on growth and yield attributes and biochemical and enzyme response of *A. dubius* cultivation under saline soils.

2. Materials and Methods

2.1. Collection of Experimental Materials

For this study, moss (*Leucobryum glaucum* (Hedw.) Ångstr.) biomass was obtained from natural rocks of the Chilla Forest Range in Rajaji National Park, Haridwar, India (29°57'55.1" N and 78°12'02.9" E). The moss attached to the rock was carefully cut using a sharp knife, and the adhering soil was carefully removed. Then, moss biomass was cut into small pieces and placed in zip-locking plastic bags for further transportation to the laboratory. For the synthesis of TiO₂ NPs, AR-grade titanium-isopropoxide was procured from Sigma–Aldrich, India, having a purity of >97%. Moreover, *A. dubius* seeds were obtained from the local market of Jwalapur, Haridwar, India (29°55'20.4" N and 78°06'19.5" E).

2.2. Biosynthesis of TiO₂ NPs and Biochar Production

The moss biomass was carefully washed in triple distilled water to remove adhering dirt and then oven-dried at 60 °C until a constant weight was obtained. The dried moss biomass was converted into a fine powder using a mechanical grinder. Further, 10 g of dried moss powder was mixed in 50 mL of triple distilled water and heated for 60 min at 80 °C. After cooling down, the solution was filtered with Whatman filter paper number 1. For the synthesis of TiO₂ NPs, 50 mL of 5 mM titanium-isopropoxide was added to 50 mL of moss extract (1:1 v/v) and continuously stirred for 8 h at 25 °C. The solution was

centrifuged for 10 min at 10,000 rpm, and formed nanoparticles were carefully separated, dried at 100 °C for 12 h, and calcinated at 570 °C using a muffle furnace for 3 h. On the other hand, the moss biochar was prepared using a slow pyrolysis process. For this, biomass was thoroughly washed and dried under sunlight to remove moisture content. The biomass was placed in a crucible disc and pyrolyzed in a muffle furnace (NSW-101, Narang Scientific, New Delhi, India) for 60 min, and the temperature was raised to 600 °C (10 °C/min). Finally, the prepared TiO₂ NPs and biochar were characterized and used for *A. dubius* cultivation experiments.

2.3. Experimental Design for Chinese Spinach Cultivation

The *A. dubius* cultivation experiments were conducted in the multipurpose laboratory of the Department of Zoology and Environmental Science, Gurukula Kangri (Deemed to be University), Haridwar, India (29°55'10.60" N and 78°07'07.90" E) during the winter season (September to October 2021). The average ambient temperature and humidity of the experimental site were 26 °C and 81%, respectively. For this purpose, the arable soil from the nearby agricultural fields was collected and filled in 25 kg capacity pre-sterilized plastic pots. A total of 19.50 kg arable soil and 0.50 kg vermicompost were filled in each pot and mixed thoroughly. This study involved a series of seven different treatments, namely T0 (arable soil only), T1 (arable soil + biochar), T2 (arable soil + TiO₂ NPs), T3 (arable soil + biochar + TiO₂ NPs), T4 (saline soil only), T5 (saline soil + biochar), T6 (saline soil + TiO₂ NPs), and T7 (saline soil + biochar + TiO₂ NPs), respectively, as depicted in Figure 1.

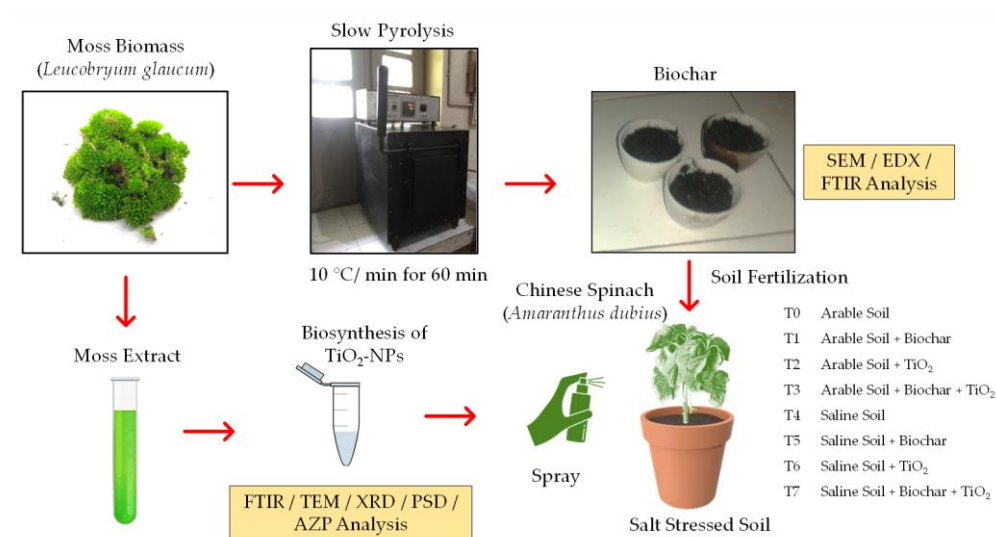


Figure 1. The layout of the experimental design used for *A. dubius* cultivation.

To achieve saline conditions in arable soil, a 150 mM NaCl (AR grade) solution was added to T4, T5, T6, and T7 treatments and mixed carefully to ensure uniform distribution of the saline solution. A 20 g dose of moss biochar per kg of soil was added to the designated pots and mixed carefully. In addition, 2.50 mg of TiO₂ NPs was added to 1000 mL of distilled water and placed in an ultrasonic water bath for 25 min to achieve uniform dissolution. The prepared solution was hand sprayed (foliar application) on *A. dubius* plants at an interval of every 10 days. For this, 25 mL of TiO₂ NPs solution was sprayed into each pot on days 10, 20, 30, and 40. Thus, a total of 100 mL of solution was sprayed into respective pots during the cultivation period. All treatments had five identical replicates to minimize experimental and analytical bias. Before their sowing, the seeds of *A. dubius* were soaked in water for 2 h and then gently dried using blotting paper to remove excess water content. Afterward, a total of three seeds were shown in each pot at a depth of 0.5 cm and covered gently with loose soil. The pots were equally watered using a borewell water supply with the help of a hand sprayer and placed under natural

sunlight conditions (16/8 h dark/light period). After germination began, the pots were watered after each third day or as per requirements to maintain appropriate soil moisture content. The first harvesting was performed on the 40th day after showing when leaves were fully matured. A total of three harvestings were performed at an interval of the fifth day to represent average plant yield. During the experiments, regular weeding and pest monitoring were performed to minimize variations due to management.

2.4. Growth, Yield, and Biochemical Analyses

The effect of TiO₂ NPs and biochar on *A. dubius* grown under saline stress was studied by analyzing the selected biochemical and enzyme responses. In this regard, the chlorophyll content (mg/g) of *A. dubius* was determined using 80% acetone extract and the spectrophotometric (Cary 60, Agilent Technologies, Santa Clara, CA, USA) method at 645 and 663 nm. Similarly, carotenoid contents (mg/g) were measured at 480, 645, and 663 nm while using acetone, chloroform, and petroleum ether as extraction reagents. Relative water content (%) of *A. dubius* was estimated via floating leaf samples on deionized water in Petri dishes for 24 h to achieve full turgidity, followed by oven drying at 80 °C to achieve constant dry weight [35]. The relative water content (%) of the plant was then calculated based on the difference between its initial hydrated state and the final dry weight, providing valuable information about the plant's water content relative to its maximum capacity for water absorption. Similarly, catalase (CAT: micromoles per minute per milligram of protein or $\mu\text{mol}/\text{min}/\text{mg P}$) activity was estimated using a 0.50 g leaf sample homogenized in a 50 mM phosphate buffer (pH: 7.8) followed by spectrophotometric estimated at 240 nm as previously described by Uma et al. [36]. Similarly, peroxidase (POD: $\mu\text{mol}/\text{min}/\text{mg P}$) activities were also determined using a 50 mM phosphate buffer, 20 mM guaiacol, 40 mM H₂O₂, and 0.10 mL extract followed by estimation at 470 nm. Moreover, superoxide dismutase (SOD: units per milligram of protein or U/mg P) contents in *A. dubius* leaves were estimated using a modified method of nitroblue tetrazolium (NBT) assay at 560 nm. In comparison, ascorbate peroxidase (APX: $\mu\text{mol}/\text{min}/\text{mg P}$) activities were recorded at 290 nm while homogenizing the sample in a 0.10 M potassium phosphate buffer (pH 7.0) [37].

2.5. Analytical and Instrumental Methods

Before its use in NP synthesis and biochar production, the moss biomass was analyzed for selected proximate and ultimate elemental analyses as percent (%). In this, moisture content, dry weight, crude protein, volatile matter, crude lipid, and total ash were determined based on the methodologies adopted by Toor et al. [38]. The ultimate analysis of selected elements (carbon, nitrogen, and oxygen) was also determined using an elemental analyzer (CE 440, Exeter Analytical Inc., Chelmsford, MA, USA). On the other hand, the functional group characteristics of synthesized TiO₂ NPs and biochar produced from moss biomass were analyzed using Fourier's transform infrared (FTIR) spectroscopy (8400S, Shimadzu, Carlsbad, CA, USA). For this, KBr pellets were used to prepare a thin disc under high pressure and then subjected to FTIR spectroscopy to scan the sample in a range of 400–4000 1/cm. The final FTIR spectra were obtained by subtracting the KBr background and 3% smoothing in order to identify the bonding modes and functional groups present in TiO₂ NPs and biochar separately. The particle size distribution of TiO₂ NPs was determined using the scattered light intensity method, while transmission electron microscopy (TEM, FEI Tecnai G2 20 S-Twin, Hillsboro, OR, USA) was used to visualize the size and morphology of NPs. The X-ray diffraction patterns of powdered NP were analyzed using an XRD instrument (D8-Advance, Bruker, Billerica, MA, USA). Also, the apparent zeta potential (AZP) of TiO₂ NPs was analyzed using a zeta potential analyzer (DelsaTMNano C, Beckman Coulter, Brea, CA, USA). Moreover, biochar obtained from the pyrolysis of moss biomass was analyzed using scanning electron microscopy (SEM; Zeiss Gemini SEM, Carl Zeiss, Oberkochen, Germany). The Biochar sample was carefully coated and subjected to SEM imaging to visualize the surface morphology. Whereas energy-dispersive X-ray

spectroscopy (EDX; Octane Eliter Plus, Mahwah, NJ, USA) analysis was simultaneously performed to understand the basic elemental composition of biochar.

2.6. Data Analysis and Software

The data generated in this study were analyzed using Microsoft Excel 365 (Microsoft Corp., Redmond, WA, USA) and OriginPro 2023b (OriginLab Corp., Northampton, MA, USA) software packages. The significant differences among treatment groups were studied based on the analysis of variance (ANOVA) while comparing the means using Tukey's post hoc test. The level of significant difference was adjusted to a 95% confidence interval or $p < 0.05$.

3. Results and Discussion

3.1. Characteristics of Moss Biomass, Synthesized TiO₂ NPs, and Biochar

3.1.1. Properties of Moss Biomass

The chemical composition of *L. glaucum* used in the present investigation is reported in Table 1. Moss moisture content was found to be $63.3 \pm 2.04\%$; it is well known that most species cannot tolerate moisture levels lower than 35% as this leads to desiccation occurrence [39]. The dry weight of *L. glaucum* ($36.7 \pm 0.31\%$) was relatively higher than the range previously set by Hoekstra et al. [40] and Alpert [39] (10–30%); this can be attributed to the type of moss species studied. Ihl and Barboza [41] found a dry weight of 17.7–31.5% for Alaska moss species, which is close but lower than observed in *L. glaucum* ($36.70 \pm 0.31\%$). This may be related to the species type and ecosystem in which it thrives. A crude protein content of $7.25 \pm 0.07\%$ was found in *L. glaucum*, thus being in the range mentioned by Orlov and Sadovnikova [42,43] (5–10%) for Bryophytes. The volatile matter content of *L. glaucum* was $38.15 \pm 1.78\%$, which was more than two-fold higher than attributed for other moss species (0.04–14.5%) [44]. A higher volatile matter production by mosses may be attributed to the attraction of flies for spore dispersal [45]. A crude lipid content of $2.41 \pm 0.04\%$ was found in *L. glaucum*; generally, such a component is scantily researched in moss species. Most attention goes to fatty acids that account for around 70% of the total lipid content of moss species [46]. Total ash content ($2.97 \pm 0.02\%$) was well below the range detected in Alaska moss species (8.1–19.6%) [41] and higher by 2–20-folds than found (0.1–1.2%) by Zacccone et al. [47]. Carbon ($49.28 \pm 2.60\%$) and nitrogen ($3.10 \pm 0.04\%$) contents detected in *L. glaucum* were higher than those reported by Klavina [48] on 16 moss species (40–43% and 0.4–2%, respectively) and in the ranges depicted by Zacccone et al. [47] (45–63% and 0.4–5.8%, respectively). On the other hand, the oxygen content of *L. glaucum* ($28.05 \pm 1.52\%$) was well below the range (48–53%) observed by Klavina [48]. CO₂ uptake (amount) directly affects the amount of oxygen produced by mosses [49]. Thus, the chemical composition of *L. glaucum* investigated in this study exhibited unique characteristics, including a relatively high dry weight, volatile matter content, and carbon and nitrogen levels, which may be influenced by the specific moss species and its ecosystem.

Table 1. Proximate and ultimate analysis results of moss biomass used in this study.

Parameter	Value
Moisture content (%)	63.30 ± 2.04
Dry weight (%)	36.70 ± 0.31
Crude protein (%)	7.25 ± 0.07
Volatile matter (%)	38.15 ± 1.78
Crude lipid (%)	2.41 ± 0.04
Total ash (%)	2.97 ± 0.02
Carbon (%)	49.28 ± 2.60
Nitrogen (%)	3.10 ± 0.04
Oxygen (%)	28.05 ± 1.52

Values are mean followed by the standard deviation of three analyses.

3.1.2. Properties of Synthesized TiO₂ NPs

The stability of synthesized NPs can be confirmed by evaluating particle size and apparent zeta potential [50]. TiO₂ NPs had a size ranging from 1 to 83 nm. At a 67 a.u. intensity (highest intensity reached), TiO₂ NPs were of 20 nm size. It is worth noting that between 60 and 67 a.u. intensity, TiO₂ NPs showed a certain size uniformity (18–22 nm) (Figure 2a,c). This indicates a specific relationship between the intensity level and the size of the nanoparticles. However, TiO₂ NPs were generally a non-uniform size. Larue et al. [51] mentioned that 4–100 nm NPs have the ability to cross plant cuticles by disrupting the wax layer. Other researchers mentioned that 3.5–20 nm NPs were likely to penetrate plants [52,53]. Zeta potential explains the potential stability of nanoparticles in a solution. The negative apparent zeta potential peak of TiO₂ NPs (around −17 mV) explains that particles were of similar charges and tended to strongly repel each other within the extract (Figure 2b). Thus, there would be a lesser tendency for TiO₂ NPs to settle down or come together in any solution (positive result). In summary, the stability of the synthesized TiO₂ NPs was confirmed through the evaluation of particle size and apparent zeta potential.

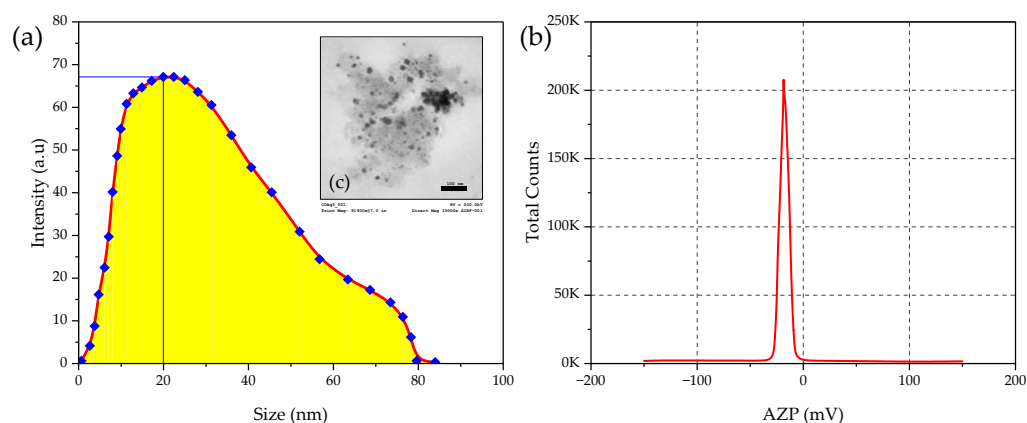


Figure 2. (a) Particle size distribution (nm), (b) apparent zeta potential (mV), and (c) TEM image of TiO₂ NPs synthesized using extract of moss biomass.

The FT-IR analysis was performed to determine the functional groups present in TiO₂ NPs synthesized using an extract of moss biomass. Positive wavelength peaks (1/cm) of absorption correspond to negative apparent peaks of IR transmittance [14]. Figure 3a shows sharp peaks at 520, 587, and 680 1/cm, referring to ring torsion of phenyl, strong C-I stretching between halo compounds, and C-H bending vibrations, respectively [54]. The peak observed at 828 1/cm can be attributed to strong C=C bending between mono- and di-substituted (alkane) compounds mostly found in carbohydrates and sugars. The peak detected at 1280 1/cm outlines the presence of collagen or amide III band components of protein. Aliphatic C-H stretching of cell wall polysaccharides can explain the peak observed at 1390 1/cm [48]. Figure 3b shows the patterns of TiO₂ NPs synthesized using an extract of moss biomass. XRD peaks observed at 2θ corresponding to 110°, 101°, 200°, 111°, 210°, 211°, 220°, 002°, 310°, and 301° plane indices indicated the crystalline structure of synthesized TiO₂ NPs. The determined results corroborate with previous reports of El-Desoky et al. [55] and Usgodaarachchi et al. [56]. Therefore, TiO₂ NPs synthesized using moss biomass extract had distinct peaks corresponding to specific chemical bonds and compounds. Additionally, XRD analysis confirmed the crystalline nature of the synthesized TiO₂ NPs.

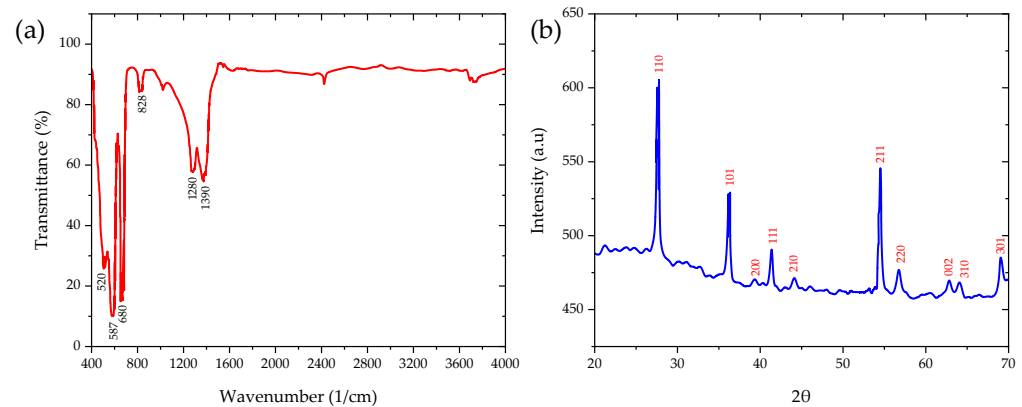


Figure 3. (a) FTIR spectra and (b) XRD patterns of TiO₂ NPs synthesized using extract of moss biomass.

3.1.3. Properties of Produced Biochar

Figure 4 shows (a) FTIR spectra, (b) EDX, and (c) SEM patterns of biochar produced from moss biomass. Four peaks were detected at 1020 (i), 1650 (ii), 1740 (iii), and 2940 (iv) 1/cm (Figure 4a) corresponding to (i) OH and C-O deformation in secondary alcohols and ethers induced by cell wall polysaccharides, (ii) amide I and C=O stretching in conjugated aryl ketones induced by proteins and phenolic compounds, (iii) C=O stretching in unconjugated ketones induced by carbohydrates, and (iv) C-H stretching in methyl and methylene groups mainly induced by lipids with contributions of proteins, carbohydrates, and phenolics, respectively [48]. SEM-EDX has been successfully used previously to evaluate the surface morphology and ultimate elemental composition of produced biochar [14]. Figure 4b depicted low amounts of calcium (Ca; 2.160%), magnesium (Mg; 2.09%), and potassium (K; 0.57%) detected at low (Mg) and moderate (Ca and K) counts. The highest ionization energy peaks were detected at low counts for carbon (C) and oxygen (O) (68.10% and 17.46%, respectively). Although C and O constituted around 85.5% of the total elements found in the produced biochar, around 9.6% of elements were not detected and may be potentially toxic elements. Therefore, more investigations should target the detection of these impurities. It is worth noting that biochar produced in this investigation had a higher C content than the one produced by Širić et al. [14] using spent mushroom substrate (68.10% and 62.06%, respectively), while the O content of the latter was higher than the former (25.10% and 17.46%, respectively). Although air oxidation is essential for the efficient increase of biochar's porosity [57], increased oxygen content can lead to biochar yield reduction [58]. Figure 2c shows visually good adsorption capacity and relative fineness of biochar produced from moss biomass. Hence, the biochar produced from moss biomass exhibited distinct chemical characteristics determined via FTIR, SEM-EDX, and SEM patterns, with specific functional groups and elemental composition identified.

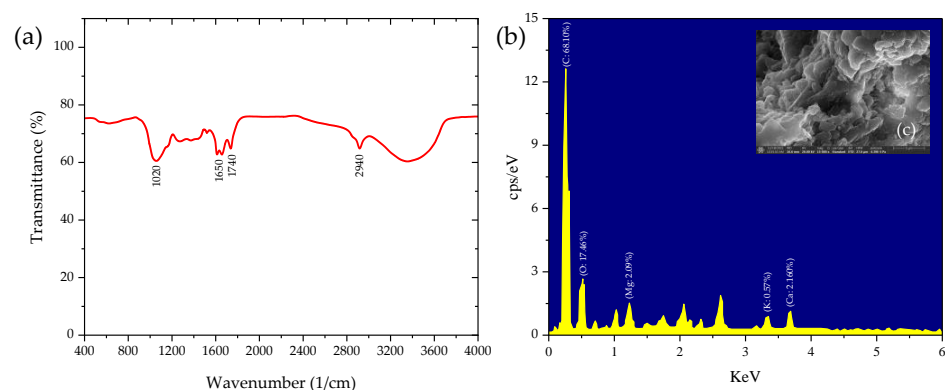


Figure 4. (a) FTIR spectra and (b,c) SEM-EDX patterns of biochar produced using moss biomass.

3.2. Effect of TiO₂ NPs and Biochar on Growth and Yield of *A. dubius*

A. dubius cultivation experiments showed that biochar mixing and foliar application of synthesized TiO₂ NPs showed a significant ($p < 0.05$) effect on growth and yield attributes (Table 2). The results showed that fresh weight in the control treatment (T0) was 31.10 g/plant, which was significantly reduced to 20.52 g/plant under saline stress (T4). However, the combined application of biochar and TiO₂ NPs application showed a significant incline in fresh weight of the T7 treatment, i.e., 30.81 (50.14%) as compared to the T4 treatment. However, the highest fresh weight (36.34 g/plant) was recorded in the T3 treatment, which had no saline stress with the combined application of moss biochar and TiO₂ NPs. A similar trend was also observed for the dry weight of *A. dubius*, i.e., maximum in T3 treatment (5.30 g/plant) while minimum in T4 treatment (3.42 g/plant). Likewise, shoot and root lengths (33.04 and 16.09 cm) were also found in the T3 treatment of non-saline soil, followed by the T7 treatment of saline soil (shoot: 28.64 and 12.54 cm). A notable observation was the average number of leaves (22.20) and leaf area (17.07 cm²/plant), which were found to be the highest in the T3 treatment. Biochar mixing helps in increasing soil nutrient composition and water-holding capacity, which later results in higher crop yields. Moreover, biochar particles added to the soil help in the improved propagation of soil microbes, which is beneficial for efficient rhizosphere association development [59]. On the other hand, foliar application of different NPs has been found to alleviate osmotic stress and reactive oxygen species (ROS) scavenging under saline-stress soils [60]. Additionally, the immobilization of excess salts via biochar prevents their uptake by plant roots, reducing ion toxicity [61]. In particular, TiO₂ NPs have been found to offer biological mechanisms through which plants can ameliorate the harmful effects of salinity and promote better crop yield [62]. Both biochar and TiO₂ NPs contribute to the improvement of soil structure. Biochar improves soil porosity, water infiltration, and aeration, while TiO₂ NPs help reduce soil compaction. The synergistic effect leads to improved root penetration and nutrient uptake, which could have promoted better plant growth.

Table 2. Effect of TiO₂ NPs and biochar application on growth and yield attributes of *A. dubius*.

Parameters	Treatments							
	T0	T1	T2	T3	T4	T5	T6	T7
Fresh weight (g/plant)	31.10 ± 1.40 b	34.05 ± 1.07 a	32.51 ± 1.16 ab	36.34 ± 2.07 a	20.52 ± 2.25 d	22.29 ± 1.09 cd	24.09 ± 0.64 c	30.81 ± 0.72 b
Dry weight (g/plant)	5.09 ± 0.15 bc	5.23 ± 0.09 b	5.16 ± 0.08 bc	5.30 ± 0.06 a	3.42 ± 0.10 e	3.45 ± 0.03 de	3.53 ± 0.07 d	4.90 ± 0.14 c
Shoot length (cm)	30.57 ± 0.90 b	33.42 ± 1.08 a	30.90 ± 0.41 b	33.04 ± 0.57 ab	17.20 ± 1.01 f	19.16 ± 0.35 e	24.75 ± 0.81 d	28.64 ± 1.30 c
Root length (cm)	14.10 ± 0.41 c	15.36 ± 0.14 b	14.28 ± 0.20 c	16.09 ± 0.24 a	7.53 ± 0.12 g	8.10 ± 0.04 f	11.03 ± 0.09 e	12.54 ± 0.17 d
Leaf number	19.00 ± 0.56 c	20.50 ± 0.42 b	19.70 ± 0.28 c	22.20 ± 0.35 a	9.80 ± 0.49 g	10.20 ± 0.50 fg	15.40 ± 0.18 e	17.50 ± 0.44 d
Leaf area (cm ² /plant)	13.80 ± 0.35 c	14.02 ± 0.12 b	14.07 ± 0.15 b	17.08 ± 0.07 a	8.10 ± 0.14 g	8.95 ± 0.26 f	10.62 ± 0.31 e	12.50 ± 0.20 d

Values are mean followed by the standard deviation of five replicates; a–g: the same letters indicate no significant difference among treatment groups at $p < 0.05$.

In a study by Odjegba and Chukwunwike [63], *A. hybridus* was grown under salinity stress of 0.10 and 0.20 M NaCl. They observed that the salinity stress resulted in a significant ($p < 0.05$) decrease in plant weight. Similarly, Amukali et al. [64] also investigated the effect of 0–150 mM NaCl on germination and seedling growth of *A. hybridus*. They observed that germination was severely impacted by 150 mM NaCl dose while shoot length (7.97 cm), root length (4.18 cm), fresh weight (2.43 g), dry weight (0.49 g), and leaf area index (1.04) were significantly declined as compared to control treatment with no NaCl amendment. Similar outcomes were reported by Menezes et al. [65] when growing *A. cruentus* under saline stress (25 mM of NaCl). They reported that the major plant growth attributes and K⁺/Na⁺ ratio were significantly decreased in saline stress treatment compared to non-saline stress treatments. Therefore, it was observed that a combination of moss biochar mixing

and foliar application of TiO₂ NPs showed a stimulatory impact on the growth and yield parameters of *A. dubius* in this study.

3.3. Effect of TiO₂ NPs and Biochar on Biochemical Response of *A. dubius*

Saline stress has deteriorating impacts on plant physiology and growth, which ultimately affects overall crop yield [66]. However, crop plants respond to saline stress by developing biochemical pathways and physiological adaptations that help them to survive high saline conditions. In this, several defense enzymes play a crucial role in plant survival. In this study, the saline stress caused by NaCl was significantly mitigated by the addition of moss biochar and TiO₂ NPs. Table 3 shows the effects of biochar and TiO₂-NP application on the biochemical and stress enzyme response of *A. dubius*. The findings showed that the chlorophyll content of *A. dubius* was significantly decreased in saline stress treatment (T4: 1.13 mg/g fwt.) compared to the control treatment (T0: 2.49 mg/g fwt.). A similar trend was observed for carotenoids (from 3.36 to 2.02 mg/g) and relative water content (from 87.01 to 72.50%). However, biochar and TiO₂-NP treatment resulted in a significant ($p < 0.05$) increase in chlorophyll, carotenoids, and relative water contents in both non-saline and saline treatments. Overall, the increasing order of these parameters was observed as: T4 < T5 < T6 < T7 < T0 < T1 < T2 < T3. On the other hand, the activities of selected plant enzymes varied significantly across the experimental treatments. SOD contents were highest in the T4 treatment, i.e., 4.05 U/mg P, which was reduced to 2.47 U/mg P in the T7 treatment. However, both CAT and SOD in non-saline stress treatments were found to be the lowest due to no specific stress. Specifically, CAT activities were highest (5.84 $\mu\text{mol}/\text{min}/\text{mg P}$) under T4 treatment, which was significantly ($p < 0.05$) reduced after the application of biochar and TiO₂ NPs. CAT acts as an important defense enzyme that helps in the breakdown of H₂O₂ molecules produced by external stresses [67]. Similarly, SOD helps in scavenging harmful superoxide radicles, which are produced by plants under saline stress [68]. Likewise, biochar and TiO₂-NP application also helped to reduce the contents of POD and APX in saline-stressed treatments, which indicates that the *A. dubius* plant could survive efficiently in these treatments. However, individual application of moss biochar and TiO₂ NPs did not show any significant ($p > 0.05$) improvement in biochemical parameters. Thus, in order to overcome the challenges of saline soils and increase *A. dubius* yields while ensuring environmental sustainability, the combined use of biochar and TiO₂ NPs offers a promising solution.

Several studies have confirmed that both biochar and NPs can ameliorate saline stress from agricultural soils [69–71]. Out of them, Farhangi-Abriz and Torabian [69] conducted laboratory experiments for French bean (*Phaseolus vulgaris* L. cv. Derakhshan) cultivation under saline-stressed soils. They found that the contents of chlorophyll were significantly reduced in saline treatments, which again increased in biochar-amended treatments. A report by Naz et al. [70] showed that foliar application of potassium mitigated saline stress conditions in *Spinacia oleracea* where activities of CAT and SOD enzymes were significantly ($p < 0.05$) affected. Moreover, González-García et al. [71] showed that foliar application of three types of nanoparticles (Se, Si, and Cu) showed a significant impact on SOD, CAT, POD, and APX activities of Bell pepper (*Capsicum* spp.) under saline stress. Therefore, as confirmed by the results of the current study, the combined use of biochar and TiO₂ NPs presents a promising and effective strategy for enhancing spinach cultivation in saline soils.

Table 3. Effect of TiO₂ NPs and biochar application on biochemical and enzyme response of *A. dubius*.

Parameters	Treatments							
	T0	T1	T2	T3	T4	T5	T6	T7
Chlorophyll content (mg/g)	2.49 ± 0.05 d	2.53 ± 0.03 c	2.94 ± 0.05 b	3.25 ± 0.07 a	1.13 ± 0.03 h	1.39 ± 0.04 g	1.87 ± 0.06 f	2.36 ± 0.05 e
Carotenoids (mg/g)	3.36 ± 0.07 a	3.42 ± 0.05 a	3.40 ± 0.06 a	3.49 ± 0.03 a	2.02 ± 0.03 e	2.23 ± 0.04 d	2.68 ± 0.03 c	2.85 ± 0.02 b
Relative water content (%)	87.01 ± 1.14 b	88.69 ± 0.64 b	89.05 ± 0.21 ab	91.40 ± 0.70 a	72.50 ± 1.63 e	73.14 ± 0.19 e	78.32 ± 0.24 d	82.10 ± 0.86 c
SOD (U/mg P)	2.20 ± 0.03 e	2.16 ± 0.02 ef	2.12 ± 0.03 f	2.04 ± 0.01 g	4.05 ± 0.04 a	3.50 ± 0.07 b	2.98 ± 0.03 c	2.47 ± 0.05 d
POD (μmol/min/mg P)	38.29 ± 0.58 e	37.65 ± 0.19 f	37.08 ± 0.35 fg	36.59 ± 0.52 g	58.72 ± 1.29 a	51.84 ± 0.91 b	48.01 ± 1.46 c	40.03 ± 2.49 d
CAT (μmol/min/mg P)	1.90 ± 0.03 e	1.82 ± 0.02 f	1.84 ± 0.04 ef	1.85 ± 0.02 ef	5.84 ± 0.07 a	5.10 ± 0.04 b	4.26 ± 0.10 c	2.93 ± 0.12 d
APX (μmol/min/mg P)	2.71 ± 0.05 e	2.66 ± 0.07 ef	2.64 ± 0.03 f	2.56 ± 0.04 g	7.45 ± 0.10 a	6.57 ± 0.09 b	4.74 ± 0.04 c	3.10 ± 0.05 d

Values are mean followed by the standard deviation of five replicates; a–g: the same letters indicate no significant difference among treatment groups at $p < 0.05$.

4. Conclusions

The findings of the present study indicated that moss biomass could act as a promising resource to produce biochar, while its extract can be used for the biosynthesis of TiO₂ NPs. The produced biochar and TiO₂ NPs were characterized for their suitability in agricultural use for *A. dubius* cultivation. The results showed a significant ($p < 0.05$) impact of the combined use of biochar and TiO₂ NPs on the growth, yield, biochemical, and stress enzyme response of *A. dubius* while alleviating saline stress. The combination of these amendments exhibited a synergistic effect, as evidenced by the significantly higher yields compared to the control group. This study suggests that moss could act as a biomass for the development of low-cost fertilizers and nanoparticles, which could benefit sustainable agriculture production. Further studies on optimization and economic feasibility of biochar and TiO₂ NP dose with unveiling the underlying mechanisms of plant, biochar, and TiO₂ NP interactions are highly recommended. Moreover, evaluating the field efficacy of the proposed method under different agro-climatic conditions and other cultivars is suggested for future works.

Author Contributions: Conceptualization, I.Š., S.A.F., P.K. (Pankaj Kumar) and E.M.E.; data curation, B.M., V.D., S.A.F., J.S. and R.S.; formal analysis, J.S., P.K. (Piyush Kumar), R.K.B. and M.G.; funding acquisition, S.K.A., L.A.A.-S. and E.M.E.; investigation, J.S., P.K. (Piyush Kumar), M.G. and P.K. (Pankaj Kumar); methodology, I.Š., S.K.A., L.A.A.-S., V.D., V.K., P.K. (Pankaj Kumar) and E.M.E.; project administration, S.K.A. and L.A.A.-S.; resources, B.M., V.K. and P.K. (Pankaj Kumar); software, S.K.A., L.A.A.-S., B.M., V.D., R.S. and R.K.B.; supervision, E.M.E.; validation, I.Š., B.M., V.K., P.K. (Piyush Kumar), R.S., R.K.B. and M.G.; visualization, I.Š., B.M., V.D., S.A.F., R.S. and R.K.B.; writing—original draft, S.A.F. and P.K. (Pankaj Kumar); writing—review and editing, I.Š., S.K.A., L.A.A.-S., B.M., V.D., V.K., J.S., P.K. (Piyush Kumar), R.S., R.K.B., M.G. and E.M.E. All authors have read and agreed to the published version of the manuscript.

Funding: This research was funded by Princess Nourah bint Abdulrahman University Researchers Supporting Project number (PNURSP2023R365), Princess Nourah bint Abdulrahman University, Riyadh, Saudi Arabia. This research was funded by the Deanship of Scientific Research at King Khalid University through the Large Groups Project under grant number (R.G.P.2/77/44).

Institutional Review Board Statement: Not applicable.

Informed Consent Statement: Not applicable.

Data Availability Statement: Not applicable.

Acknowledgments: The authors extend their appreciation to Princess Nourah bint Abdulrahman University Researchers Supporting Project number (PNURSP2023R365), Princess Nourah bint Abdulrahman University, Riyadh, Saudi Arabia. The authors extend their appreciation to the Deanship of Scientific Research at King Khalid University for funding this work through the Large Groups Project

under grant number (R.G.P.2/77/44). All individuals included in this section have consented to the acknowledgement.

Conflicts of Interest: The authors declare no conflict of interest.

References

- Grande, F.; Tucci, P. Titanium Dioxide Nanoparticles: A Risk for Human Health? *Mini-Rev. Med. Chem.* **2016**, *16*, 762–769. [CrossRef]
- Shi, H.; Magaye, R.; Castranova, V.; Zhao, J. Titanium Dioxide Nanoparticles: A Review of Current Toxicological Data. *Part. Fibre Toxicol.* **2013**, *10*, 15. [CrossRef] [PubMed]
- Gupta, N.; Rai, D.B.; Jangid, A.K.; Kulhari, H. Use of Nanotechnology in Antimicrobial Therapy. In *Methods in Microbiology*; Elsevier: Amsterdam, The Netherlands, 2019; Volume 46, pp. 143–172. ISBN 9780128149928.
- Aravind, M.; Amalanathan, M.; Mary, M.S.M. Synthesis of TiO₂ Nanoparticles by Chemical and Green Synthesis Methods and Their Multifaceted Properties. *SN Appl. Sci.* **2021**, *3*, 409. [CrossRef]
- Gonfa, Y.H.; Tessema, F.B.; Bachheti, A.; Tadesse, M.G.; Eid, E.M.; Abou Fayssal, S.; Adelodun, B.; Choi, K.S.; Širić, I.; Kumar, P.; et al. Essential Oil Composition of Aerial Part of *Pluchea ovalis* (Pers.) DC., Silver Nanoparticles Synthesis, and Larvicidal Activities against Fall Armyworm. *Sustainability* **2022**, *14*, 15785. [CrossRef]
- Verma, V.; Al-Dossari, M.; Singh, J.; Rawat, M.; Kordy, M.G.M.; Shaban, M. A Review on Green Synthesis of TiO₂ NPs: Photocatalysis and Antimicrobial Applications. *Polymers* **2022**, *14*, 1444. [CrossRef] [PubMed]
- Sett, A.; Gadewar, M.; Sharma, P.; Deka, M.; Bora, U. Green Synthesis of Gold Nanoparticles Using Aqueous Extract of *Dillenia indica*. *Adv. Nat. Sci. Nanosci. Nanotechnol.* **2016**, *7*, 025005. [CrossRef]
- Srujana, S.; Anjamma, M.; Alimuddin, Singh, B.; Dhakar, R.C.; Natarajan, S.; Hechhu, R. A Comprehensive Study on the Synthesis and Characterization of TiO₂ Nanoparticles Using *Aloe vera* Plant Extract and Their Photocatalytic Activity against MB Dye. *Adsorpt. Sci. Technol.* **2022**, *2022*, 7244006. [CrossRef]
- Roopan, S.M.; Bharathi, A.; Prabhakarn, A.; Abdul Rahuman, A.; Velayutham, K.; Rajakumar, G.; Padmaja, R.D.; Lekshmi, M.; Madhumitha, G. Efficient Phyto-Synthesis and Structural Characterization of Rutile TiO₂ Nanoparticles Using *Annona squamosa* Peel Extract. *Spectrochim. Acta A Mol. Biomol. Spectrosc.* **2012**, *98*, 86–90. [CrossRef]
- Velayutham, K.; Rahuman, A.A.; Rajakumar, G.; Santhoshkumar, T.; Marimuthu, S.; Jayaseelan, C.; Bagavan, A.; Kirthi, A.V.; Kamaraj, C.; Zahir, A.A.; et al. Evaluation of Catharanthus Roseus Leaf Extract-Mediated Biosynthesis of Titanium Dioxide Nanoparticles against *Hippobosca maculata* and *Bovicola ovis*. *Parasitol. Res.* **2012**, *111*, 2329–2337. [CrossRef]
- Vimala, A.; Sahaya Sathish, S.; Thamizharasi, T.; Palani, R.; Vijayakanth, P.; Kavitha, R. Moss (Bryophyte) Mediated Synthesis and Characterization of Silver Nanoparticles from *Campylopus flexuosus* (Hedw.) Bird. *J. Pharm. Sci. Res.* **2017**, *9*, 292–297.
- Akhatova, F.; Konnova, S.; Kryuchkova, M.; Batasheva, S.; Mazurova, K.; Vikulina, A.; Volodkin, D.; Rozhina, E. Comparative Characterization of Iron and Silver Nanoparticles: Extract-Stabilized and Classical Synthesis Methods. *Int. J. Mol. Sci.* **2023**, *24*, 9274. [CrossRef]
- Hernandez-Soriano, M.C.; Kerré, B.; Kopittke, P.M.; Horemans, B.; Smolders, E. Biochar Affects Carbon Composition and Stability in Soil: A Combined Spectroscopy-Microscopy Study. *Sci. Rep.* **2016**, *6*, 25127. [CrossRef] [PubMed]
- Širić, I.; Eid, E.M.; Taher, M.A.; El-Morsy, M.H.E.; Osman, H.E.M.; Kumar, P.; Adelodun, B.; Abou Fayssal, S.; Mioč, B.; Andabaka, Ž.; et al. Combined Use of Spent Mushroom Substrate Biochar and PGPR Improves Growth, Yield, and Biochemical Response of Cauliflower (*Brassica oleracea* var. *botrytis*): A Preliminary Study on Greenhouse Cultivation. *Horticulturae* **2022**, *8*, 830. [CrossRef]
- Tomczyk, A.; Sokołowska, Z.; Boguta, P. Biochar Physicochemical Properties: Pyrolysis Temperature and Feedstock Kind Effects. *Rev. Environ. Sci. Biotechnol.* **2020**, *19*, 191–215. [CrossRef]
- Shaaban, A.; Se, S.-M.; Dimin, M.F.; Juoi, J.M.; Mohd Husin, M.H.; Mitan, N.M.M. Influence of Heating Temperature and Holding Time on Biochars Derived from Rubber Wood Sawdust via Slow Pyrolysis. *J. Anal. Appl. Pyrolysis* **2014**, *107*, 31–39. [CrossRef]
- Zhang, J.; Liu, J.; Liu, R. Effects of Pyrolysis Temperature and Heating Time on Biochar Obtained from the Pyrolysis of Straw and Lignosulfonate. *Bioresour. Technol.* **2015**, *176*, 288–291. [CrossRef]
- Maximize Market Research Amaranth Market: Global Industry Analysis and Forecast (2022–2029). Available online: <https://www.maximizemarketresearch.com/market-report/global-amaranth-market/81299/> (accessed on 13 August 2023).
- Raiger, H.L.; Phogat, B.S.; Dua, R.P.; Sharma, S.K. *Improved Varieties and Cultivation Practices of Grain Amaranth*; Indian Council of Agricultural Research, Krishi Bhavan: New Delhi, India, 2009.
- Sarker, U.; Islam, M.T.; Oba, S. Salinity Stress Accelerates Nutrients, Dietary Fiber, Minerals, Phytochemicals and Antioxidant Activity in *Amaranthus tricolor* Leaves. *PLoS ONE* **2018**, *13*, e0206388. [CrossRef]
- Sarker, U.; Oba, S. Protein, Dietary Fiber, Minerals, Antioxidant Pigments and Phytochemicals, and Antioxidant Activity in Selected Red Morph *Amaranthus* Leafy Vegetable. *PLoS ONE* **2019**, *14*, e0222517. [CrossRef]
- Sarker, U.; Oba, S. Salinity Stress Enhances Color Parameters, Bioactive Leaf Pigments, Vitamins, Polyphenols, Flavonoids and Antioxidant Activity in Selected *Amaranthus* Leafy Vegetables. *J. Sci. Food Agric.* **2019**, *99*, 2275–2284. [CrossRef]
- Estrada, Y.; Fernández-Ojeda, A.; Morales, B.; Egea-Fernández, J.M.; Flores, F.B.; Bolarín, M.C.; Egea, I. Unraveling the Strategies Used by the Underexploited Amaranth Species to Confront Salt Stress: Similarities and Differences with *Quinoa* Species. *Front. Plant Sci.* **2021**, *12*, 604481. [CrossRef]

24. Bellache, M.; Allal Benfekih, L.; Torres-Pagan, N.; Mir, R.; Verdeguer, M.; Vicente, O.; Boscaiu, M. Effects of Four-Week Exposure to Salt Treatments on Germination and Growth of Two *Amaranthus* Species. *Soil. Syst.* **2022**, *6*, 57. [[CrossRef](#)]
25. Hoang, L.H.; De Guzman, C.C.; Cadiz, N.M.; Tran, D.H. Physiological and Phytochemical Responses of Red Amaranth (*Amaranthus tricolor* L.) and Green Amaranth (*Amaranthus dubius* L.) to Different Salinity Levels. *Legume Res. An. Int. J.* **2019**, *43*, 206–211. [[CrossRef](#)]
26. Sardar, H.; Khalid, Z.; Ahsan, M.; Naz, S.; Nawaz, A.; Ahmad, R.; Razzaq, K.; Wabaidur, S.M.; Jacquard, C.; Širić, I.; et al. Enhancement of Salinity Stress Tolerance in Lettuce (*Lactuca sativa* L.) via Foliar Application of Nitric Oxide. *Plants* **2023**, *12*, 1115. [[CrossRef](#)] [[PubMed](#)]
27. Gour, T.; Sharma, A.; Lal, R.; Heikrujam, M.; Gupta, A.; Agarwal, L.K.; Chetri, S.P.K.; Kumar, R.; Sharma, K. Amelioration of the Physio-Biochemical Responses to Salinity Stress and Computing the Primary Germination Index Components in Cauliflower on Seed Priming. *SSRN Electron. J.* **2022**, *9*, e14403. [[CrossRef](#)]
28. El-Shal, R.M.; El-Naggar, A.H.; El-Beshbeshy, T.R.; Mahmoud, E.K.; El-Kader, N.I.A.; Missaui, A.M.; Du, D.; Ghoneim, A.M.; El-Sharkawy, M.S. Effect of Nano-Fertilizers on Alfalfa Plants Grown under Different Salt Stresses in Hydroponic System. *Agriculture* **2022**, *12*, 1113. [[CrossRef](#)]
29. Zhang, S. Mechanism of Migration and Transformation of Nano Selenium and Mitigates Cadmium Stress in Plants. Master's Thesis, Shandong University, Jinan, China, 2019.
30. Francis, D.V.; Sood, N.; Gokhale, T. Biogenic CuO and ZnO Nanoparticles as Nanofertilizers for Sustainable Growth of *Amaranthus hybridus*. *Plants* **2022**, *11*, 2776. [[CrossRef](#)]
31. Cai, Y.; Yuan, B.; Ma, X.; Fang, G.; Zhou, D.; Gao, J. Foliar Application of SiO₂ and ZnO Nanoparticles Affected Polycyclic Aromatic Hydrocarbons Uptake of Amaranth (*Amaranthus tricolor* L.): A Metabolomics and Typical Statistical Analysis. *SSRN Electron. J.* **2022**, *833*, 155258. [[CrossRef](#)]
32. Situmeang, Y.P.; Suarta, M.; Irianto, I.K.; Andriani, A.A.S.P.R. Biochar Bamboo Application on Growth and Yield of Red Amaranth (*Amaranthus tricolor* L.). *IOP Conf. Ser. Mater. Sci. Eng.* **2018**, *434*, 012231. [[CrossRef](#)]
33. Jiang, S.; Dai, G.; Zhou, J.; Zhong, J.; Liu, J.; Shu, Y. An Assessment of Integrated Amendments of Biochar and Soil Replacement on the Phytotoxicity of Metal(Loid)s in Rotated Radish-Soya Bean-Amaranth in a Mining Acidic Soil. *Chemosphere* **2022**, *287*, 132082. [[CrossRef](#)]
34. Daryabeigi Zand, A.; Tabrizi, A.M.; Heir, A.V. Co-Application of Biochar and Titanium Dioxide Nanoparticles to Promote Remediation of Antimony from Soil by *Sorghum bicolor*: Metal Uptake and Plant Response. *Heliyon* **2020**, *6*, e04669. [[CrossRef](#)]
35. González, L.; González-Vilar, M. Determination of Relative Water Content. In *Handbook of Plant Ecophysiology Techniques*; Kluwer Academic Publishers: Dordrecht, The Netherlands, 2006; pp. 207–212.
36. Uma, S.; Karthic, R.; Kalpana, S.; Backiyarani, S. A Comparative Assessment of Photosynthetic Pigments and Defense Enzymes in Ex Vitro and In Vitro Propagated Plants of Banana (*Musa* spp.). *Biocatal. Agric. Biotechnol.* **2023**, *51*, 102799. [[CrossRef](#)]
37. Upadhyay, P.; Tewari, A.K.; Punetha, H. Biochemical Estimation of Polyphenol and Peroxidases in Resistant Sources against White Rust Disease of Rapeseed Mustard In-Cited by *Albugo candida*. *Pharma Innov. J.* **2023**, *12*, 4964–4974.
38. Toor, S.S.; Reddy, H.; Deng, S.; Hoffmann, J.; Spangsmark, D.; Madsen, L.B.; Holm-Nielsen, J.B.; Rosendahl, L.A. Hydrothermal Liquefaction of *Spirulina* and *Nannochloropsis salina* under Subcritical and Supercritical Water Conditions. *Bioresour. Technol.* **2013**, *131*, 413–419. [[CrossRef](#)] [[PubMed](#)]
39. Alpert, P. The Limits and Frontiers of Desiccation-Tolerant Life. *Integr. Comp. Biol.* **2005**, *45*, 685–695. [[CrossRef](#)]
40. Hoekstra, F.A.; Golovina, E.A.; Buitink, J. Mechanisms of Plant Desiccation. *Trends Plant Sci.* **2001**, *6*, 431–438. [[CrossRef](#)]
41. Ihl, C.; Barboza, P.S. Nutritional Value of Moss for Arctic Ruminants: A Test with Muskoxen. *J. Wildl. Manag.* **2007**, *71*, 752–758. [[CrossRef](#)]
42. Arnon, D.I. Copper Enzymes in Isolated Chloroplasts. Polyphenoloxidase in *Beta vulgaris*. *Plant Physiol.* **1949**, *24*, 1–15. [[CrossRef](#)]
43. Orlov, D.S.; Sadovnikova, L.K. Soil Organic Matter and Protective Functions of Humic Substances in the Biosphere. In *Use of Humic Substances to Remediate Polluted Environments: From Theory to Practice*; Springer: Dordrecht, The Netherlands, 2005; ISBN 978-1-4020-3252-3.
44. Ryde, I.; Davie-Martin, C.L.; Li, T.; Naursgaard, M.P.; Rinnan, R. Volatile Organic Compound Emissions from Subarctic Mosses and Lichens. *Atmos. Environ.* **2022**, *290*, 119357. [[CrossRef](#)]
45. McCuaig, B.; Dufour, S.C.; Raguso, R.A.; Bhatt, A.P.; Marino, P. Structural Changes in Plastids of Developing *Splachnum ampullaceum* Sporophytes and Relationship to Odour Production. *Plant Biol.* **2015**, *17*, 466–473. [[CrossRef](#)]
46. Resemann, H.C.; Lewandowska, M.; Gießmann, J.; Feussner, I. Membrane Lipids, Waxes and Oxylipins in the Moss Model Organism *Physcomitrella patens*. *Plant Cell Physiol.* **2019**, *60*, 1166–1175. [[CrossRef](#)]
47. Zaccone, C.; Miano, T.M.; Shotyk, W. Qualitative Comparison between Raw Peat and Related Humic Acids in an Ombrotrophic Bog Profile. *Org. Geochem.* **2007**, *38*, 151–160. [[CrossRef](#)]
48. Klavina, L. Composition of Mosses, Their Metabolites and Environmental Stress Impacts. Ph.D. Thesis, University of Latvia, Riga, Latvia, 2018.
49. Serk, H.; Nilsson, M.B.; Bohlin, E.; Ehlers, I.; Wieloch, T.; Olid, C.; Grover, S.; Kalbitz, K.; Limpens, J.; Moore, T.; et al. Global CO₂ Fertilization of Sphagnum Peat Mosses via Suppression of Photorespiration during the Twentieth Century. *Sci. Rep.* **2021**, *11*, 24517. [[CrossRef](#)] [[PubMed](#)]

50. Ramdath, S.; Mellem, J.; Mbatha, L.S. Anticancer and Antimicrobial Activity Evaluation of Cowpea-Porous-Starch-Formulated Silver Nanoparticles. *J. Nanotechnol.* **2021**, *2021*, 5525690. [[CrossRef](#)]
51. Larue, C.; Castillo-Michel, H.; Sobanska, S.; Trcera, N.; Sorieul, S.; Cécillon, L.; Ouerdane, L.; Legros, S.; Sarret, G. Fate of Pristine TiO₂ Nanoparticles and Aged Paint-Containing TiO₂ Nanoparticles in Lettuce Crop after Foliar Exposure. *J. Hazard. Mater.* **2014**, *273*, 17–26. [[CrossRef](#)] [[PubMed](#)]
52. Palocci, C.; Valletta, A.; Chronopoulou, L.; Donati, L.; Bramosanti, M.; Brasili, E.; Baldan, B.; Pasqua, G. Endocytic Pathways Involved in PLGA Nanoparticle Uptake by Grapevine Cells and Role of Cell Wall and Membrane in Size Selection. *Plant Cell Rep.* **2017**, *36*, 1917–1928. [[CrossRef](#)]
53. Cai, L.; Cai, L.; Jia, H.; Liu, C.; Wang, D.; Sun, X. Foliar Exposure of Fe₃O₄ Nanoparticles on *Nicotiana benthamiana*: Evidence for Nanoparticles Uptake, Plant Growth Promoter and Defense Response Elicitor against Plant Virus. *J. Hazard. Mater.* **2020**, *393*, 122415. [[CrossRef](#)] [[PubMed](#)]
54. Movasaghi, Z.; Rehman, S.; Ur Rehman, I. Fourier Transform Infrared (FTIR) Spectroscopy of Biological Tissues. *Appl. Spectrosc. Rev.* **2008**, *43*, 134–179. [[CrossRef](#)]
55. El-Desoky, M.M.; Morad, I.; Wasfy, M.H.; Mansour, A.F. Synthesis, Structural and Electrical Properties of PVA/TiO₂ Nanocomposite Films with Different TiO₂ Phases Prepared by Sol–Gel Technique. *J. Mater. Sci. Mater. Electron.* **2020**, *31*, 17574–17584. [[CrossRef](#)]
56. Usgodaarachchi, L.; Thambiliyagodage, C.; Wijesekera, R.; Vigneswaran, S.; Kandanapitiye, M. Fabrication of TiO₂ Spheres and a Visible Light Active α -Fe₂O₃/TiO₂-Rutile/TiO₂-Anatase Heterogeneous Photocatalyst from Natural Ilmenite. *ACS Omega* **2022**, *7*, 27617–27637. [[CrossRef](#)]
57. Sun, Z.; Dai, L.; Lai, P.; Shen, F.; Shen, F.; Zhu, W. Air Oxidation in Surface Engineering of Biochar-Based Materials: A Critical Review. *Carbon Res.* **2022**, *1*, 32. [[CrossRef](#)]
58. Bakshi, S.; Banik, C.; Laird, D.A. Estimating the Organic Oxygen Content of Biochar. *Sci. Rep.* **2020**, *10*, 13082. [[CrossRef](#)] [[PubMed](#)]
59. Lehmann, J.; Rillig, M.C.; Thies, J.; Masiello, C.A.; Hockaday, W.C.; Crowley, D. Biochar Effects on Soil Biota—A Review. *Soil. Biol. Biochem.* **2011**, *43*, 1812–1836.
60. Tomar, R.S.; Kataria, S.; Jajoo, A. Behind the Scene: Critical Role of Reactive Oxygen Species and Reactive Nitrogen Species in Salt Stress Tolerance. *J. Agron. Crop Sci.* **2021**, *207*, 577–588. [[CrossRef](#)]
61. Shaheen, S.M.; Mosa, A.; Natasha; Arockiam Jeyasundar, P.G.S.; Hassan, N.E.E.; Yang, X.; Antoniadis, V.; Li, R.; Wang, J.; Zhang, T.; et al. Pros and Cons of Biochar to Soil Potentially Toxic Element Mobilization and Phytoavailability: Environmental Implications. *Earth Syst. Environ.* **2023**, *7*, 321–345. [[CrossRef](#)]
62. Gohari, G.; Mohammadi, A.; Akbari, A.; Panahirad, S.; Dadpour, M.R.; Fotopoulos, V.; Kimura, S. Titanium Dioxide Nanoparticles (TiO₂ NPs) Promote Growth and Ameliorate Salinity Stress Effects on Essential Oil Profile and Biochemical Attributes of *Dracocephalum moldavica*. *Sci. Rep.* **2020**, *10*, 912. [[CrossRef](#)]
63. Odjegba, V.J.; Chukwunwike, I.C. Physiological Responses of *Amaranthus hybridus* L. Under Salinity Stress. *Niger. J. Life Sci.* **2022**, *5*, 242–252. [[CrossRef](#)]
64. Amukali, O.; Obadoni, B.O.; Mensah, J.K. Effects of Different NaCl Concentrations on Germination and Seedling Growth of *Amaranthus hybridus* and *Celosia argentea*. *Afr. J. Environ. Sci. Tech.* **2015**, *9*, 301–306. [[CrossRef](#)]
65. Menezes, R.V.; De Azevedo Neto, A.D.; Ribeiro, M.d.O.; Cova, A.M.W. Growth and Contents of Organic and Inorganic Solutes in Amaranth under Salt Stress. *Pesqui. Agropecu. Trop.* **2017**, *47*, 22–30. [[CrossRef](#)]
66. Ferreira, J.; Sandhu, D.; Liu, X.; Halvorson, J. Spinach (*Spinacea oleracea* L.) Response to Salinity: Nutritional Value, Physiological Parameters, Antioxidant Capacity, and Gene Expression. *Agriculture* **2018**, *8*, 163. [[CrossRef](#)]
67. Seymen, M. Comparative Analysis of the Relationship between Morphological, Physiological, and Biochemical Properties in Spinach (*Spinacea oleracea* L.) under Deficit Irrigation Conditions. *Turk. J. Agric. For.* **2021**, *45*, 55–67. [[CrossRef](#)]
68. Das, K.; Roychoudhury, A. Reactive Oxygen Species (ROS) and Response of Antioxidants as ROS-Scavengers during Environmental Stress in Plants. *Front. Environ. Sci.* **2014**, *2*, 53. [[CrossRef](#)]
69. Farhangi-Abriz, S.; Torabian, S. Effect of Biochar on Growth and Ion Contents of Bean Plant under Saline Condition. *Environ. Sci. Pollut. Res.* **2018**, *25*, 11556–11564. [[CrossRef](#)] [[PubMed](#)]
70. Naz, T.; Mazhar Iqbal, M.; Tahir, M.; Hassan, M.M.; Rehmani, M.I.A.; Zafar, M.I.; Ghafoor, U.; Qazi, M.A.; EL Sabagh, A.; Sakran, M.I. Foliar Application of Potassium Mitigates Salinity Stress Conditions in Spinach (*Spinacia oleracea* L.) through Reducing NaCl Toxicity and Enhancing the Activity of Antioxidant Enzymes. *Horticulturae* **2021**, *7*, 566. [[CrossRef](#)]
71. González-García, Y.; Cárdenas-Álvarez, C.; Cadenas-Pliego, G.; Benavides-Mendoza, A.; Cabrera-de-la-Fuente, M.; Sandoval-Rangel, A.; Valdés-Reyna, J.; Juárez-Maldonado, A. Effect of Three Nanoparticles (Se, Si and Cu) on the Bioactive Compounds of Bell Pepper Fruits under Saline Stress. *Plants* **2021**, *10*, 217. [[CrossRef](#)] [[PubMed](#)]

Disclaimer/Publisher’s Note: The statements, opinions and data contained in all publications are solely those of the individual author(s) and contributor(s) and not of MDPI and/or the editor(s). MDPI and/or the editor(s) disclaim responsibility for any injury to people or property resulting from any ideas, methods, instructions or products referred to in the content.